

# Unsupervised Lane-Change Identification for On-Ramp Merge Analysis in Naturalistic Driving Data

Lars Klitzke\*, Kay Gimm\*, Carsten Koch<sup>†</sup> and Frank Köster\*

**Abstract**—Connected and Automated Vehicles (CAVs) are envisioned to transform the future industrial and private transportation sectors. Due to the complexity of the systems, functional verification and validation of safety aspects are essential before the technology merges into the public domain. In recent years, a scenario-driven approach has gained acceptance for CAVs emphasizing the requirement of a solid data basis of scenarios.

The large-scale research facility Test Bed Lower Saxony (TFNDS) enables the provision of substantial information for a database of scenarios on motorways. For that purpose, however, the scenarios of interest must be identified and categorized in the collected trajectory data. This work addresses this problem and proposes a framework for on-ramp scenario identification that also enables for scenario categorization and assessment. The efficacy of the framework is shown with a dataset collected on the TFNDS.

**Index Terms**—Highway On-Ramp Merging, Naturalistic Driving Data, Unsupervised Learning, Connected and Automated Vehicles

## I. INTRODUCTION

The transport sector has a significant impact on the environment. In 2017, the mobility sector emitted 18.5% of the total greenhouse gases (GHG) in Germany [1]. Especially with the Paris agreement in 2016, the automotive industry faces a massive challenge by reducing the GHG of their fleets to become carbon neutral. Although a rethinking of mobility is required for this, there are several technologies that may help to reach this goal.

In recent years, researchers focussed on the topic of connected and automated vehicles (CAV) due to the availability of the required sensors for environment perception and infrastructure technology for communication. The communication between vehicles (V2V) or vehicles and infrastructure (V2I) enables CAV to conduct their driving task more efficiently and thus reducing the impact on the environment [2]. Moreover, the technology enables a safer [3], more energy efficient [4] and comfortable driving experience.

Before those technologies merge into the market, a homologation is required. This is addressed by several research projects such as PEGASUS, ENABLE-3S and their successors VVM and SET Level<sup>1</sup>. The systems' functional correctness needs to be verified, which is hard to accomplish

\*Lars Klitzke, Kay Gimm and Frank Köster are with the German Aerospace Center (DLR), Institute of Transportation Systems, Braunschweig, Germany {lars.klitzke, kay.gimm, frank.koester}@dlr.de.

<sup>†</sup>Carsten Koch is with the Hochschule Emden/Leer, University of Applied Sciences, Emden, Germany carsten.koch@hs-emden-leer.de.

<sup>1</sup>www.pegasusprojekt.de/en, www.enable-s3.eu, www.vvm-projekt.de/en, https://setlevel.de/en

with real-world drivings only [5]. Hence, scenario-driven simulation-based testing is applied extensively throughout the development cycle [6], [7].

An interesting scenario is the on-ramp merging scenario with a vehicle merging onto the mainline from an on-ramp lane. Merging vehicles can affect the overall traffic flow, and those situations can become critical in case of, *e.g.*, a short on-ramp lane, high occupancy of the mainline, occluded field-of-view, or high relative velocities. Furthermore, vehicles participating in this scenario often have to collaborate to resolve the situation, making this scenario interesting in mixed traffic situations of CAV and traditional vehicles. For such analysis, however, an extensive catalog of scenarios is essential [8], with data from the real-world providing valuable information.

The Germany Aerospace Center (DLR) constructed a large-scale research facility named Test Bed Lower Saxony (TFNDS) to test technology in the context of automated and connected driving. The camera-based surveillance infrastructure on the motorway A39 with a length of 7km allows for tracking objects on the motorway and providing information about a vehicle under test (VUT) such as the pose, dimension, vehicle type and its environment in specific scenarios. For scenario-based analysis of a VuT and situation assessment, *e.g.*, in terms of criticality using SSMs such as the time to collision (TTC) [7] or post encroachment time (PET) [9], however, the identification of these scenarios, also referred to as scenario mining [10], is mandatory.

### A. Related Work

The identification of scenarios is a broadly discussed topic in the research community for several years and becomes even more relevant with the recent shift to a scenario-driven validation approach. In the following, a short overview of recent activities in this domain is given.

For the identification of scenarios in trajectory data various approaches exists in literature to tackle this problem. In general, the aim is to find certain characteristic time intervals in a multivariate time-series. Supervised learning methods such as the Support Vector Machine (SVM) and Artificial Neuronal Network (ANN) were proposed by [11], [12], [13], [14]. The inherent drawback of these approaches is, however, the training of (hyper)parameter based on ground truth data.

A comparative study for scenario identification is conducted by [15] with a rule-based, supervised (Recurrent Neuronal Network (RNN)) and unsupervised learning ( $k$ -NN & Dynamic Time Warping (DTW)) method. Although the RNN is superior to the unsupervised learning method, it is

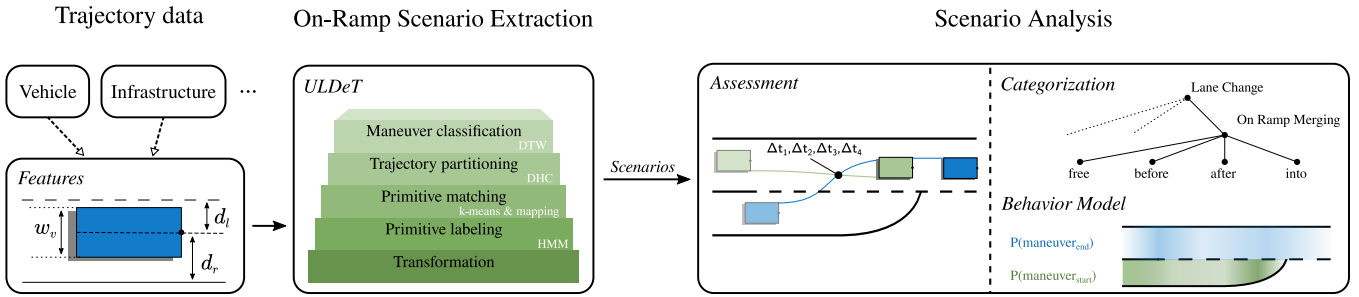


Fig. 1: The proposed framework for on-ramp scenario identification and analysis. The trajectory data can be supplied by various sources and just needs to be converted to provide the required *Features* which are used for scenario extraction with *ULDeT*. The scenarios are assessed, categorized and the on-ramp behavior is characterized in the *Scenario analysis* module.

more prone to sensor noise [15] which is inevitable in real-world data.

An alternative to supervised learning-based methods are approaches for clustering, *i.e.*, unsupervised learning methods. [16] slices time-series into chunks based on artificially created signals with empirically defined parameters and Agglomerative Hierarchical Clustering (AHC). For finding different variants of lane changes, the final interpretation of clusters is performed manually. This problem is inherent with non-deterministic unsupervised learning methods such as AHC, Random Forest Clustering [17] or Hidden Markov Model (HMM) [18] and post-processing steps are required to recover the semantics either manually or automatically [19]. For instance, [20] employs regular expressions to find maneuvers in the trajectory data after clustering it into symbolic states. However, they show that crafting the patterns has a significant impact on identification accuracy.

## B. Contribution

The contribution of this work is threefold. The first is a framework for the identification of on-ramp merging scenarios in naturalistic driving data provided by the Test Bed Lower Saxony (TFNDS) to contribute setting up an extensive dataset of on-ramp merging scenarios for testing. For that purpose, the result of a previous work [18] is adapted where the focus was on the identification of lane-changes from a vehicle-oriented point of view. That is, information about the environment are derived using on-board systems.

The second contribution is the automatic categorization of merging scenarios according to the occupancy of the mainline using the surrogate safety measure (SSM) PET which also allows to identify critical scenarios. These are of special interest for further simulation-based testing.

The last contribution is related to the behavior of drivers on the on-ramp lane. These insights are valuable especially in the context of mixed-traffic of CAV and non-automated vehicles. This work shed light on where vehicles start and finish the merging maneuver and proposes a model, derived from empirical data, to represent this behavior which can be employed to generate on-ramp merging maneuvers.

## C. Paper Structure

The remaining paper is structured as follows. In Section II the proposed methodology for on-ramp scenario identification and analysis is presented with emphasis on trajectory data from the TFNDS. In Section III follows an evaluation of the on-ramp identification method and an analysis of on-ramp scenarios on the TFNDS. Finally, the work concludes with a summary and outlook on future work in Section IV.

## II. METHODOLOGY

For the identification and analysis of of on-ramp merges in naturalistic driving data provided by the TFNDS, this work employs the framework presented in [18] which is based on multiple unsupervised learning methods and extends it with further modules as depicted Fig. 1. In the following, the framework and the fundamental assumptions on a lane-change are briefly revisited for the sake of completeness and the new modules for scenario analysis are presented.

### A. Lane Change Maneuver

A lane-change is in this work partitioned into multiple states, the *driving primitives*. This allows to break down the complexity of a lane-change maneuver to more trivial driving actions which can be identified more easily [18].

From a lane-oriented point of view, the maneuver can be unambiguously divided into four states as depicted in Fig. 2, which is a slightly modified version as presented in [18]. That is, the state *Change* denotes the transition from the source lane to the target lane until the majority of the vehicle is on the target lane. The state *Depart* is equal to the state *Change* but in the opposite direction relative to the lane. This division does not only allow to model the behavior of lane-change more precisely on the driving primitive level but also allows extract the lane-change straightforward after the identification.

For the association of a vehicle's position to a driving primitive, information about the vehicle's relative position w.r.t the road is required. In Fig. 2 it is evident that the state is dependent on the distance to the left lane marking since this is a lane change to the left. Hence, for a right lane change the distance to the next right lane marking is required. If we assume that the reference point is the front center position (indicated by the block dot) and the state *Cross*

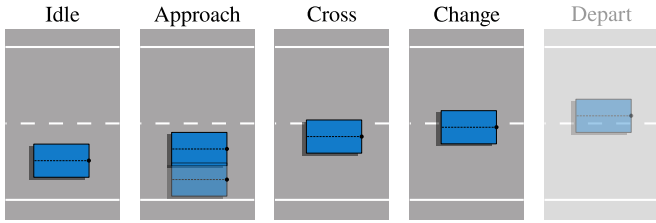


Fig. 2: A lane-change is represented with four driving primitives [18]. From a lane-oriented point of view the state Depart is equal to Change but in the opposite direction.

should really denote that the vehicle crosses the marking, than the vehicle’s width is also relevant. Indeed, only those three features are required for the follow-up processing. Also note that the data source is irrelevant which is also denoted on the left side in Fig. 1 showing the required *features* that needs to be provided by any trajectory data source, *e.g.*, vehicles equipped with appropriate sensors, test beds such as the TFNDS or even drones [21].

### B. Feature estimation for Test Bed Lower Saxony data

Since the aim of this work is to analyse on-ramp merging scenarios on the TFNDS, the trajectory data need to be pre-processed to provide the features as depicted in Fig. 1.

As already mentioned in the Section I the TFNDS provides information such as the pose, dimension and velocity of objects. Hence, the width of the object is available. But, the distances to the lane markings need to be estimated since access on in-vehicle systems is not available.

For that purpose, a high precision digital map of the TFNDS is employed which is represented in the OpenDrive<sup>2</sup> format (see Fig. 3). A road network is represented with so called *reference lines*. Each reference line represents a certain segment of the network and is linked to other segments by their unique ID. The shape of roads associated with a reference line is represented with other geometric objects such as lines, spirals or arcs. For the sake of simplicity, however, this work uses an abstraction level on top of this with all geometric objects of the road network being represented by lines in the GEOJSON format as so called *LineString* objects. That is, each geometric object is represented by a series of points. In Fig. 3 the on-ramp section of the TFNDS near Cremlingen is depicted with the *reference lines* in blue and their associated *lane borders* in green.

For the estimation of the lateral distances to the next lane borders, the first step is to derive an aggregated version of the digital map (see Fig. 4). In this aggregated version, each lane border is only represented as a single geometric object that consists of multiple segments and lanes are associated to either the on-ramp or the motorway section. This allows to filter objects based on their associated road and enables to pick only trajectories being on the on-ramp lane. For that purpose, preselected reference lines and other connected reference lines are identified and all intersecting lane borders

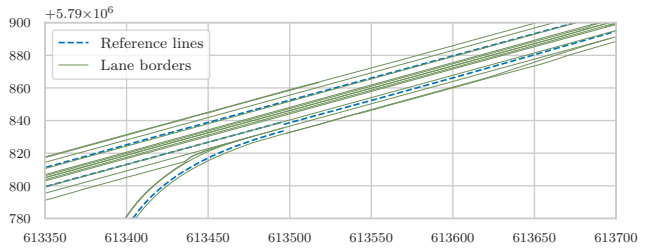


Fig. 3: The digital map of the on-ramp at Cremlingen of the Test-Bed Lower Saxony. Reference lines (dashed blue) represent sections of the road network and lane borders (green) specific geometric objects.

associated with these reference lines are merged. The *start* depicted in Fig. 4 marker denotes the intersection point between the on-ramp and motorway lane used in Section III-D as reference point to estimate the relative trajectory length.

The aggregated map is used to estimate the the distances to the left  $d_l$  and right  $d_r$  lane marking according to [22]. That is, the orthogonal distances from all lane marking segments to the object are estimated, whereas the reference point on the object is the front center position provided by the camera-based object detection system. The distances  $d_l$  and  $d_r$  are equal to the distances to the two nearest lane marking segments. The trajectory data of the TFNDS is now preprocessed to provide the required features for lane change detection.

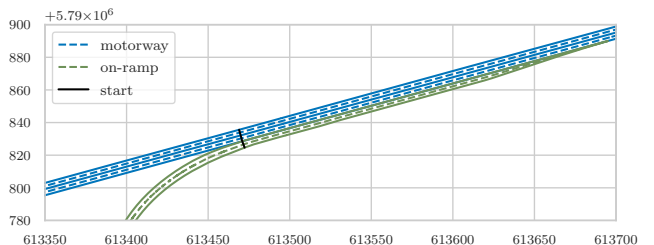


Fig. 4: The aggregated version of the digital map only contains lanes related to the road with the on-ramp lane. The lanes are either associated with the **motorway** or **on-ramp**.

### C. On-Ramp Merging Scenario identification

Based on the aforementioned features that are provided by a trajectory data source such as the TFNDS, the data processing pipeline ULDeT (Unsupervised Lane change Detection) presented in an earlier work [18] is employed for scenario identification which is briefly described in the following.

Since the aim is to identify only trajectories performing an on-ramp merge and the motorway contains two lanes, the first step is to filter trajectories. That is, only trajectories starting on the on-ramp lane are considered and processed with *ULDeT*.

The identification of lane changes with *ULDeT* is based on the representation of that maneuver with the driving

<sup>2</sup><https://www.asam.net/standards/detail/opensdrive/>

primitives as discussed in Section II-A. For partitioning trajectories into the driving primitives depicted in Fig. 2 a time-invariant HMM with Gaussian emission is employed since it allows to model the hidden states (the driving primitives) of a certain system (the lane change) and the transitions between them according to the information this system emits (the features in Fig. 1). Although the HMM model parameter could be defined manually, they are estimated using a data-driven approach by employing the Baum-Welch algorithm [23] and a dataset. Note that the model parameters are taken from a previous work [18] since the dataset used in this work is solely for on-ramp merges and thus, does only contain left lane changes which lead to instability in clustering.

Note that the features depicted in Fig. 1 are not used by the HMM but a transformation is applied first by *ULDeT* to ensure that the clustering with the HMM work for different vehicles and lanes. That is, the features are the distance from the vehicle's center to the lane's center and a marker indicating the vehicle is crossing a lane marker.

The Viterbi algorithm is employed to cluster a time-series with the HMM. [23] The result is a time-series of labels mapping each point in time to the most likely HMM state (driving primitive). The next step is, based on the position of the vehicle relative to the lane, to derive the primitive direction, since follow-up steps require this information, and the correct primitive label, because the association between a driving primitive and a HMM state may change for consecutive runs.

A trajectory might contain multiple lane changes. Therefore, Divisive Hierarchical Clustering (DHC) is employed to partition the time-series of primitive labels into sequences. Note that this might not be relevant for the use-case of on-ramp identification addressed in this work, but allows to identify scenarios where the ego-vehicle merges onto the leftmost lane on multi-lane motorways (assuming right-hand driving). For the final classification of a sequence, which is a time series of driving primitive labels, a pattern matching approach is employed. Instead of using regular expressions as in [20], DTW is employed to match the sequence with manually defined patterns for the scenarios of interest and the most likely one is chosen. The benefit of this approach is that the sequence must not follow the defined pattern closely which is, however, the case for regular expressions.

Although we proposed a method for scenario extraction based on the lateral position change in previous work, this work extracts the maneuver interval solely based on the primitive, because we are interested in the interval where the vehicle is transitioning from the source to the target lane. That is, the maneuver starts at the last occurrence of the *Approach* state before the actual transition and ends at the first occurrence of the *Approach* state after the transition.

#### D. Scenario Assessment

The identified on-ramp merging scenarios are processed in the *Scenario Analysis* for situation assessment, scenario categorization and behavior modeling as depicted in Fig. 1. For the assessment of scenarios in terms of the criticality

so called surrogate safety measures (SSMs) are typically utilized. For lane changes, the PET is broadly used [24], [9] for that purpose and thus chosen for this work since it not only allows to assess a certain situation but also provides information for further scenario categorization.

The PET is the time difference between the first object leaving and the second object entering a conflict area [25]. In the following, the first is denoted as the *ego vehicle* and the latter as the *challengers* as defined in [26]. The lower the PET between two objects, the higher the potential criticality. In this specific case, the conflicting areas are derived by finding the four intersection points  $P_c = p_1, \dots, p_4$  of the ego vehicle's rear left and front left edges to the rear right and front right edges of the challengers  $c \in C = \{c_1, c_2, \dots\}$ . Then, the differences between the arrival times  $\Delta T_c = \Delta t_1^c, \dots, \Delta t_4^c$  of the ego-vehicle  $t_{ego}(p)$  and challenger  $t_c(p)$  to the intersection points  $P_c$  are derived as  $\Delta T_c = \{t_{ego}(p) - t_c(p) | p \in P_c\}$ . The  $PET_{ego}(c), c \in C$  between the ego vehicle and challenger  $c$  is defined in (1) with the minimum signed time difference between the arrival times of both vehicles. The estimated PET of scenarios can be employed to find critical scenarios as exemplarily shown in Section III.

$$PET_{ego}(c) = \{\Delta t | \Delta t \in \Delta T_c \wedge |\Delta t| = \min |\Delta T_c|\} \quad (1)$$

#### E. Scenario Categorization

An on-ramp scenario can be further categorized according to the challengers [9]. In this work, only the challengers on the mainline are considered for categorization at that point in time where the second vehicle reaches the conflict zone. Hence, an on-ramp scenario is in this work specialized into four subtypes *free*, *in front*, *behind* and *into* as depicted in Fig. 5.

For this categorization, the PET of each scenario is employed since the sign of the PET denotes the order of entering and leaving the conflict zone. The PET from (1) is positive if the ego vehicles arrives the intersection point after the challenger and negative vice versa. Hence, a scenario is classified as *behind* or *in front* if there is only one challenger  $C = \{c\}$  and  $PET_{ego}(c) > 0$  or  $PET_{ego}(c) < 0$  respectively. If there are at least two challengers  $C = \{c_1, c_2, \dots\}$  and  $\exists c \in C : PET_{ego}(c_1) > 0 \wedge \exists c \in C : PET_{ego}(c_1) < 0$  the lane-change is classified as *into*. If there is no challenger on the target lane, the lane-change is classified as *free*. Note that this work assumes that there is no collision between challengers and the ego vehicle.

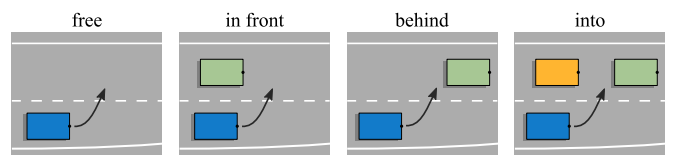


Fig. 5: An on-ramp merging scenario is specialized into four classes by considering the location of challengers on the target lane.



Fig. 6: Example images of the dataset visualized in Fig. 3 showing the on-ramp at Cremlingen of the Test Bed lower Saxony. The dataset depicted in Fig. 7 used in this work is collected in that area.

### F. On-Ramp Merging Behavior

The identification of on-ramp merging scenarios allow to derive behavioral models of the drivers, which can be employed to generate trajectories for more extensive simulation-based testing, *e.g.*, in Carla [27] or SUMO [28]. This is especially of interest in the context of mixed traffic of CAV and traditional vehicles since CAV have to predict the behavior in this situations. In this work, a model is derived based on a set of scenarios to represent the start and end position for on-ramp merging maneuvers. Note that the trajectory generation is out-of-scope of this work.

Since the aim is to generate the start and end position of new on-ramp merges, a probabilistic model is derived that can be employed for sampling. As stated by [29], the inversion method is appropriate for that task if the cumulative distribution function (cdf) of a certain event and a random variable  $r \in [0, 1]$  is given. In the following, the start and end positions are represented as distances relative to the starting position depicted in Fig. 4 and normalized according to the length of the on-ramp lane. Due to this, the term offset is used in the following. That is, a maneuver end offset of greater than one means that the maneuver ends behind the on-ramp lane. This normalization also allows to generate trajectories for different length's of on-ramp lanes and thus enables to compare the behavior for different on-ramp lane situations.

The cdf  $F(x)$  of the starting offsets  $x$  is derived empirically from the identified maneuvers, which inverse  $x = F(r)^{-1}$  is employed for sampling. Linear interpolation is used for modeling. To ensure that maneuvers end behind their start position, the maneuver lengths is employed and it is assumed that the maneuver lengths is dependent on the start offset. Due to this, the on-ramp lane is clustered into  $n$  partitions and for each partition, the cdfs of the maneuver length relative to the on-ramp lane are derived. Note that this approach can generate end positions that overshoot the actual distribution of end positions in that partition.

Let  $O$  be the set of all maneuver start offsets which is

divided into  $n$  partitions  $o_1, o_2, \dots, o_n$ . That is, the trajectory starting offsets of  $o_i$  are within the interval  $[\frac{i-1}{n}; \frac{i}{n})$ . For each partition, the cdfs  $G_i(l)$  is derived empirically for the the maneuver length  $l$ . For sampling new maneuvers, the inverse  $l = G_i^{-1}(r)$  are determined that maps the random variable  $r$  onto maneuver lengths  $l$ . [29]

The characterized models  $\{F(x), G_1(x), \dots, G_n(x)\}$  can be employed to generate the start and end point of new on-ramp maneuvers. For that purpose, assuming  $r_o$  is uniformly sampled from  $[0, 1]$ , the start offset is estimated with  $o = F(r_o)^{-1}$ . Then, the maneuver length  $l$  is sampled from the cdf  $G_i(r_l)^{-1}$  of the  $i$ th partition with  $i = \lceil 10o \rceil = 1, \dots, 9$  according to a second random variable  $r_l \in [0, 1]$  which is added to the start offset. This approach is applied in Section III-D on identified scenarios of the TFNDS.

## III. EXPERIMENTS

In the following section the proposed approach for on-ramp merging identification is evaluated with a dataset of the TFNDS. The extracted scenarios are the basis for further analysis.

### A. Dataset

The data used for the evaluation and analysis are collected at the on-ramp region at Cremlingen near Braunschweig in Germany, which is part of the TFNDS. The region is covered by four camera masts equipped with two pairs of stereo cameras. In Fig. 6 a sample image per camera is shown; row-wise from the top left to the bottom right. For the first and last camera mast, only the stereo camera pair pointing to the on-ramp is shown. The data was collected on three different days and various daytimes. Note that the used sampling strategy was to collect snippets of 90 seconds each 300 seconds. Due to this, only trajectories are considered in the analysis having a length greater than half of the on-ramp lane's length to remove clipped trajectories. The total number of trajectories in the dataset meeting this criteria is 2465 with 2339 objects

associated with the motorway lanes and 126 with the on-ramp lane. The distribution of the observed objects over the day is depicted in Fig. 7.

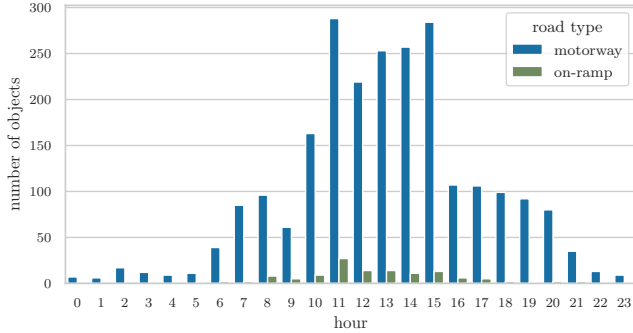


Fig. 7: Distribution of the observed objects on a per-hour basis in the dataset. The objects are associated to either the on-ramp lanes or the motorway lanes.

### B. Scenario Identification Evaluation

To evaluate the performance of the framework for on-ramp merging identification, the dataset needs to be processed with the presented framework. Therefore, only objects driving on the on-ramp are considered and the lane-change intervals are extracted.

For the 126 objects on the on-ramp lane, 119 merging scenarios are correctly and 7 incorrectly identified by the framework. The framework’s accuracy in lane-change identification is thus 94.44%.

It turns out that the framework fails in lane-change identification if a lane-change starts at the end of the on-ramp lane so that the object crosses both lane marking. This is depicted in Fig. 8 showing the relation between the start and end positions of all lane-changes and the trajectory start (sizes of markers). Note that all positions in Fig. 8 are relative to the start of the lane depicted in Fig. 4 as described in Section II-F.

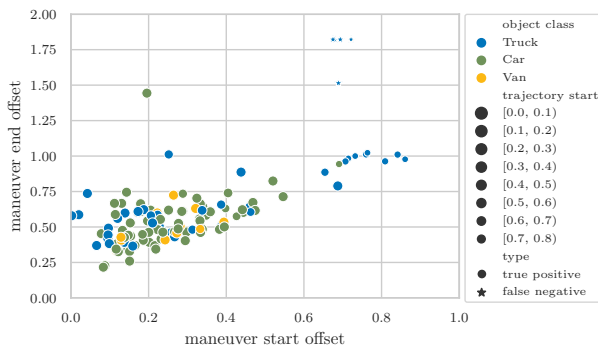


Fig. 8: Overview of the correctly (●) and incorrectly (★) identified on-ramp merges start and end offsets with object classes (color-encoded) and the trajectories start offset (marker size).

It is evident from Fig. 8 that the difference between correctly and incorrectly identified lane-changes is the end offset. That is, lane-changes starting at the end of the on-ramp lane with a start offset greater than 0.6 and ending beyond it with an end offset greater 1.4 are not identified. The start position of the trajectory has no influence in this case since all trajectories start offsets of the not identified scenarios are within  $[0.6, 0.8)$  but there are also correctly identified scenarios ( $n = 9$ ) with the same trajectory starting offset.

### C. Scenario Assessment

The Assessment module depicted in Fig. 1 uses the PET to relate the ego-vehicle on the on-ramp lane to challengers on the target lane. This enables to, e.g., find critical scenarios, i.e. scenarios with a low PET between the ego-vehicle and a challenger.

The PET distribution for the scenario categories *behind*, *in front* and *into* is depicted in Fig. 9. Note that the category *free* is missing since there is no challenger on the mainline. For the category *into* the sum of PETs values is used to represent each scenario with a single value which is related to the SSM metric accepted gap time.

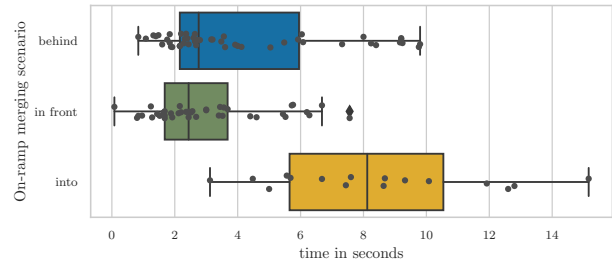


Fig. 9: Distribution of the PET time for all identified on-ramp scenarios of type *behind* and *in front* and the accepted gap time for *into*.

Fig. 9 shows that vehicles tend to merge onto the mainline quite close behind another vehicle with 50% having a PET lower than 4.0 seconds and 25% lower than 2.6 seconds. For the *into* type the PET is uniformly distributed within  $[5.0; 15.1]$  seconds and a mean of  $9.7 \pm 2.9$  seconds. The gap between a vehicle merging in front of another vehicle is even closer than for the *behind* class with 50% having a PET lower than 3.0 seconds and 25% lower than 2.0 seconds. Noteworthy is the situation with a PET of 0.08 seconds and thus denotes a near-crash situation. This can be verified in Fig. 10 showing the situation where the ego vehicle starts the lane-change maneuver and one second later. In that scenario, a vehicle (in blue) merges onto the mainline which is occupied by a truck (in green). Although the PET indicates that the scenario is critical, a “look into the future” shows that the situation becomes uncritical since the gap between both vehicles increases.

### D. Merging Behavior

The robust identification of lane-changes allow to derive behavioral models of the drivers for on-ramp merges which

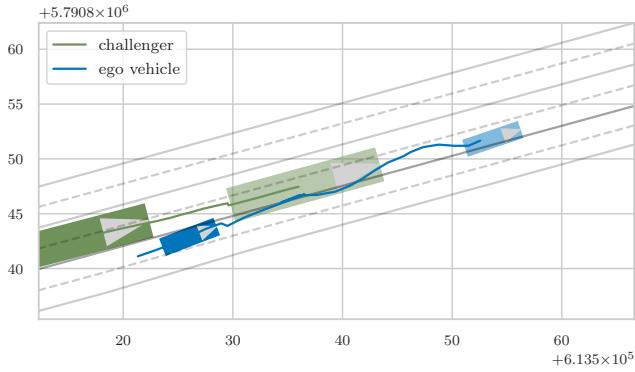


Fig. 10: The identified critical on-ramp scenario at the start of the lane change maneuver and one second later.

can be employed to generate trajectories for more extensive simulation-based testing. The identified scenarios are used to characterize the model described in Section II-F.

At first, the empirical cdf for the maneuver start offset  $F(x)$  is derived based on the identified maneuvers. In Fig. 11 the estimated cdf is depicted with the cdf of a uniform distribution as comparison.

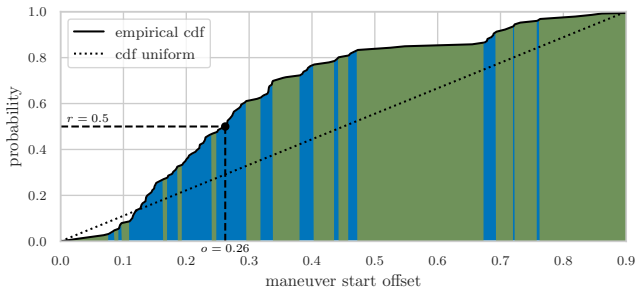


Fig. 11: The empirical cdf compared with a uniform distribution of start offsets with a sampling example of  $r = 0.5$ . The green areas denote under- and blue an overrepresented start offsets compared to a uniform distribution.

The areas in green denote start offsets that are under- and in blue overrepresented w.r.t the uniform distribution. It is evident from Fig. 11 that maneuver tend to start at the beginning of the on-ramp lane in this dataset. This is also denoted with the example of  $r = 0.5$  which is mapped to a maneuver start of 0.26, *i.e.* the likelihood for a maneuver start offset lower equal 0.26 is 0.5. This is contrary to our expectations since the acceleration lane is typically used to adapt the driving speed to the vehicles on the mainline. Hence, vehicles on the acceleration lane should stay as long as the possible on that lane. This is not the case in this dataset with only 4.21% of maneuvers starting in the last quarter and 16.19% in the second half of the lane of which are 80% trucks, 15% cars and 5% vans (see Fig. 8). Note that the models are not derived for each object type independently due to the lack of data and is part of further work.

The next step for maneuver generation is to characterize each partition's model  $G_i(x)$  for the maneuver length (see

Fig. 12). Therefore, the number of partitions need to be defined. A lower partition size may lead to partitions with no associated maneuvers and a higher partition may generate maneuver end offsets that are larger as in the original dataset. Thus, the partition size should as low as possible. For the available dataset, a partition size of 0.1 and thus  $n = 9$  partitions, due to a maximum start offset of 0.86, yield sufficient results since a lower value lead to empty partitions. The estimated cdfs for each partition is depicted in Fig. 12 with the number of samples. It is noteworthy that the gaps in Fig. 8 are also visible in Fig. 12 for the 8th and 9th partition. But, since linear interpolation is used, values in the gaps can be sampled although they are not present in the original distribution. The evaluation of more accurate kernel density estimators is subject for further works.

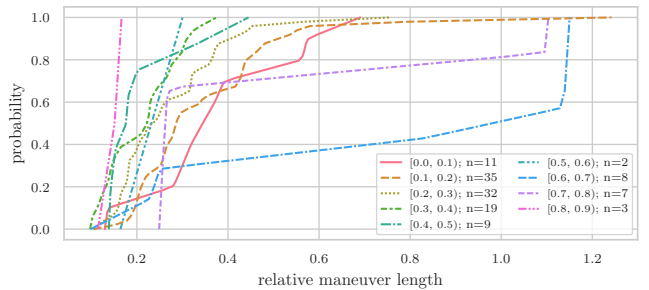


Fig. 12: The empirical cdf for each partition that is employed to sample on-ramp maneuver lengths.

As described in Section II-F the characterized models  $\{F(x), G_1(x), \dots, G_n(x)\}$  can be employed to generate the start and end point of new on-ramp maneuvers. In Fig. 13 the distribution of generated maneuvers ( $n = 1000$ ) is depicted showing the feasibility of the approach to sample appropriate maneuvers. Furthermore, the cdf of the generated start offsets is depicted in the same way as for Fig. 11. The influence of the interpolation method for the cdf is represented in two ways. At first, the blue area in the cdf has increased and secondly maneuver start offsets are clearly visible in the scatterplot with an offset greater 0.6 that are not part of the original dataset.

#### IV. CONCLUSION

A scenario-based validation approach for CAV demands information from real-world drivings such as naturalistic driving studies or field operational tests on specific proving grounds. This data need to be annotated to find scenarios of interest such as on-ramp merging scenarios.

This work addresses this issue and proposed a framework for the identification and analysis of on-ramp scenarios using unsupervised learning methods. It was shown that data from the TFNDS can be easily adopted to use *ULDeT*, which was proposed in a previous work [18], for on-ramp merging scenarios extraction with an accuracy of 94.44%. But the results also show that the method fails to identify maneuvers that start at the end of a the merging lane. The extracted scenarios are further categorized and assessed using the PET.

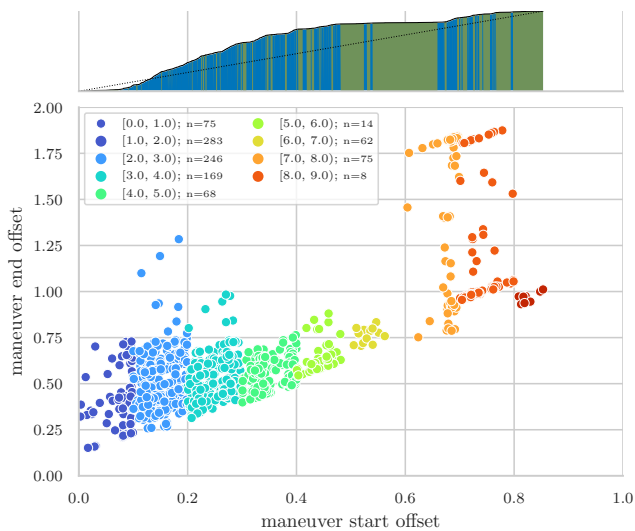


Fig. 13: The start and end offsets of generated maneuvers ( $n = 1000$ ) using the derived models from the dataset.

Furthermore, the maneuver behavior in terms of the start and end position is analysed.

In follow-up works a more comprehensive dataset will be employed to further analyze the behavior of the ego vehicle and challengers in on-ramp merging scenarios. Furthermore, the maneuver behavior models will be derived for each object type individually since trucks seem to behave differently than cars. Moreover, the approach for maneuver identification is adapted for other scenarios and integrated into a distributed data processing pipeline for scenario mining.

## REFERENCES

- [1] J. Günther, H. Lehmann, P. Nuss, and K. Purr, *Resource-efficient Pathways Towards Greenhouse-gas-neutrality-RESCUE: Summary Report*. Umweltbundesamt, 2019.
- [2] P. Kopelias, E. Demiridi, K. Vogiatzis, A. Skabardonis, and V. Zafropoulou, "Connected & autonomous vehicles – Environmental impacts – A review," *Science of The Total Environment*, vol. 712, p. 135237, 2020.
- [3] A. Papadoulis, M. Qaddus, and M. Imprialou, "Evaluating the safety impact of connected and autonomous vehicles on motorways," *Accident Analysis & Prevention*, vol. 124, pp. 12–22, 2019.
- [4] T. Guan and C. W. Frey, "Predictive energy efficiency optimization of an electric vehicle using traffic light sequence information\*," in *2016 IEEE International Conference on Vehicular Electronics and Safety (ICVES)*, 2016, pp. 1–6.
- [5] H. Winner, K. Lemmer, T. Form, and J. Mazzege, *PEGASUS—First Steps for the Safe Introduction of Automated Driving*. Switzerland: Springer International Publishing, 2018, ch. Vehicle Systems and Technologies Development, pp. 185–195.
- [6] S. Hallerbach, Y. Xia, U. Eberle, and F. Köster, "Simulation-based identification of critical scenarios for cooperative and automated vehicles," *SAE Intl. J CAV*, vol. 1, pp. 93–106, 04 2018.
- [7] C. Neurohr, L. Westhofen, M. Butz, M. H. Bollmann, U. Eberle, and R. Galbas, "Criticality analysis for the verification and validation of automated vehicles," *IEEE Access*, vol. 9, pp. 18 016–18 041, 2021.
- [8] W. Damm, E. Möhlmann, T. Peikenkamp, and A. Rakow, "A formal semantics for traffic sequence charts," in *Principles of Modeling*. Springer, 2018, pp. 182–205.
- [9] W. Qi, W. Wang, B. Shen, and J. Wu, "A modified post encroachment time model of urban road merging area based on lane-change characteristics," *IEEE Access*, vol. 8, pp. 72 835–72 846, 2020.
- [10] H. Elrofai, J. Paardekooper, E. d. Gelder, S. Kalisvaart, and O. Op den Camp, "Streetwise: scenario-based safety validation of connected automated driving," 2018.
- [11] P. Kumar, M. Perrollaz, S. Lefèvre, and C. Laugier, "Learning-based approach for online lane change intention prediction," in *2013 IEEE Intelligent Vehicles Symposium (IV)*, 2013, pp. 797–802.
- [12] R. Izquierdo, I. Parra, J. Muñoz-Bulnes, D. Fernández-Llorca, and M. A. Sotelo, "Vehicle trajectory and lane change prediction using ANN and SVM classifiers," in *2017 IEEE 20th International Conference on Intelligent Transportation Systems (ITSC)*, 2017, pp. 1–6.
- [13] S. Ramyar, A. Homaifar, A. Karimodini, and E. Tunstel, "Identification of anomalies in lane change behavior using one-class SVM," in *2016 IEEE International Conference on Systems, Man, and Cybernetics (SMC)*, Oct 2016, pp. 004 405–004 410.
- [14] N. Monot, X. Moreau, A. Benine-Neto, A. Rizzo, and F. Aioun, "Comparison of rule-based and machine learning methods for lane change detection," in *2018 21st International Conference on Intelligent Transportation Systems (ITSC)*, Nov 2018, pp. 198–203.
- [15] A. Erdogan, B. Ugranli, E. Adali, A. Sentas, E. Mungan, E. Kaplan, and A. Leitner, "Real-World Maneuver Extraction for Autonomous Vehicle Validation: A Comparative Study," in *2019 IEEE Intelligent Vehicles Symposium (IV)*, June 2019, pp. 267–272.
- [16] F. Montanari, R. German, and A. Djanatliev, "Pattern recognition for driving scenario detection in real driving data," in *2020 IEEE Intelligent Vehicles Symposium (IV)*, 2020, pp. 590–597.
- [17] F. Kruber, J. Wurst, and M. Botsch, "An Unsupervised Random Forest Clustering Technique for Automatic Traffic Scenario Categorization," in *2018 21st International Conference on Intelligent Transportation Systems (ITSC)*, Nov 2018, pp. 2811–2818.
- [18] L. Klitzke, C. Koch, and F. Köster, "Identification of Lane-Change Maneuvers in Real-World Drivings With Hidden Markov Model and Dynamic Time Warping," in *2020 IEEE 23rd International Conference on Intelligent Transportation Systems (ITSC)*, 2020, pp. 1–7.
- [19] W. Wang, J. Xi, and D. Zhao, "Driving Style Analysis Using Primitive Driving Patterns With Bayesian Nonparametric Approaches," *IEEE Transactions on Intelligent Transportation Systems*, vol. 20, no. 8, pp. 2986–2998, Aug 2019.
- [20] P. Elspas, J. Langner, M. Aydinbas, J. Bach, and E. Sax, "Leveraging regular expressions for flexible scenario detection in recorded driving data," in *2020 IEEE International Symposium on Systems Engineering (ISSE)*, 2020, pp. 1–8.
- [21] J. Bock, R. Krajewski, T. Moers, S. Runde, L. Vater, and L. Eckstein, "The ind dataset: A drone dataset of naturalistic road user trajectories at german intersections," in *2020 IEEE Intelligent Vehicles Symposium (IV)*, 2020, pp. 1929–1934.
- [22] A. Kasmi, D. Denis, R. Aufrere, and R. Chapuis, "Map matching and lanes number estimation with openstreetmap," in *2018 21st International Conference on Intelligent Transportation Systems (ITSC)*, 2018, pp. 2659–2664.
- [23] J. A. Bilmes *et al.*, "A gentle tutorial of the EM algorithm and its application to parameter estimation for Gaussian mixture and hidden Markov models," *International Computer Science Institute*, vol. 4, no. 510, p. 126, 1998.
- [24] H. Behbahani and N. Nadimi, "A framework for applying surrogate safety measures for sideswipe conflicts," *International Journal for Traffic & Transport Engineering*, vol. 5, no. 4, pp. 371–383, 2015.
- [25] D. Gettman and L. Head, "Surrogate safety measures from traffic simulation models," *Transportation Research Record*, vol. 1840, no. 1, pp. 104–115, 2003.
- [26] H. Weber, J. Bock, J. Klimke, C. Roesener, J. Hiller, R. Krajewski, A. Zlocki, and L. Eckstein, "A framework for definition of logical scenarios for safety assurance of automated driving," *Traffic Injury Prevention*, vol. 20, no. sup1, pp. S65–S70, 2019.
- [27] A. Dosovitskiy, G. Ros, F. Codevilla, A. Lopez, and V. Koltun, "CARLA: An open urban driving simulator," in *Proceedings of the 1st Annual Conference on Robot Learning*, ser. Proceedings of Machine Learning Research, S. Levine, V. Vanhoucke, and K. Goldberg, Eds., vol. 78. PMLR, 13–15 Nov 2017, pp. 1–16.
- [28] M. Behrisch, L. Bieker, J. Erdmann, and D. Krajzewicz, "SUMO – Simulation of Urban MOBility: An Overview," in *SIMUL 2011*, S. . U. of Oslo Aida Omerovic, R. I. R. T. P. D. A. Simoni, and R. I. R. T. P. G. Bobashev, Eds. ThinkMind, Oktober 2011.
- [29] R. C. Larson and A. R. Odoni, *Urban operations research*, 1981, no. Monograph.